KSCE Journal of Civil Engineering (2016) 20(5):1747-1758
DOI 10.1007/s12205-015-0268-5

Geotechnical Engineering
pISSN 1226-7988, eISSN 1976-3808
www.springer.com/12205

Stress-strain Behaviour and Shear Strength of Municipal Solid Waste (MSW)

Xiulei Li* and Jianyong Shi**

Received May 20, 2014/Revised September 18, 2014, 2nd: February 9, 2015/Accepted August 7, 2015/Published Online October 30, 2015

Abstract

An understanding of the stress-strain behaviour of Municipal Solid Waste (MSW) is important in landfill design and stability analysis of landfill slopes. A series of triaxial compression tests were carried out on reconstituted MSW specimens. The effect of stress path on the drained stress-strain response and shear strength of MSW were investigated. For the compression stress paths of $\Delta\sigma_3 \geq 0$, a straight-lined increase section and an upward curvature are observed in the stress-strain curves of MSW; the upward curvature results from the fibrous constituents (primarily plastic and paper) reinforcing the waste matrix; the hardening points defined in stress-strain curves are used as failure criterion to calculate the strength parameters of MSW. For the compression stress paths of $\Delta\sigma_3 < 0$, the stress-strain responses of MSW exhibit a rapidly increasing section towards a slowly increasing section without upward curvature; the development of fibrous reinforcement is not enough due to the reduction of confining stress σ_3; the failure points defined in stress-strain curves are also used as failure criterion to calculate the strength parameters of MSW. A new method to estimate MSW strength parameters is proposed in this study. The differences of MSW friction angle are very small for different stress path tests. However, the cohesions obtained in compression stress path tests of $\Delta\sigma_3 < 0$ are much smaller than that in conventional triaxial compression tests.

Keywords: *municipal solid waste, triaxial tests, stress path, stress-strain behaviour, shear strength*

1. Introduction

MSW is a heterogeneous material, and its stress-strain behaviour depends on various factors, such as composition, density, moisture content, spatial distribution of constituents and age. The stress-strain behaviour of MSW is a main consideration for design of landfill liner, stability analysis of foundation and slope, leachate circulation, and design of cover system (Dixon and Jones, 2005). Recently, the stability of landfill slopes has been received considerable attention due to several high-profile failures of large municipal landfills. The examples include the Cincinnati landfill failure in Ohio, USA in 1996 (Eid *et al.*, 2000), the Doña Juana landfill failure in Bogotà, Colombia in 1997 (Hendron *et al.*, 1999), the Payatas landfill failure in Manilla, Philippines in 2000 (Merry *et al.*, 2005), the Bandung landfill failure in West Java province, Indonesia in 2005 (Kölsch *et al.*, 2005). Not only had these accidents destroyed the local environment, but also caused huge economic losses and casualties. Meanwhile, these landfill failures reflect the fact that many engineering problems have not been recognized recently.

At present, a lot of data on stress-strain behaviour of MSW has been reported in the published literature, mostly based on conventional triaxial compression tests (Grisolia *et al.*, 1995; Vilar and Carvalho 2004; Singh *et al.*, 2009; Reddy *et al.*, 2011; Karimpour-Fard *et al.*, 2011; Zekkos *et al.*, 2012) and direct shear tests (Gabr and Valero 1995; Pelkey *et al.*, 2001; Gabr *et al.*, 2007; Zekkos *et al.*, 2010). The stress-strain responses of MSW obtained by the above type tests are significantly different. In conventional triaxial compression tests, all the stress-strain curves of MSW generally have the same shape, with an initial downward curvature at small strains followed by almost a linear increase section to an upwards curvature without reaching any peak or tending to an asymptotic value. In direct shear tests, all the stress-deformation curves of MSW exhibit a downward curvature towards peak shear stress or asymptotic conditions. Because of no peak shear stress or asymptotic value in conventional triaxial test results, an axial strain is often used as friction criterion to calculate the shear strength parameters of MSW (normally 10-30% of axial strain). The upward curvature is not observed in direct shear tests, which can be attributed to the fact that the horizontal shearing surface is roughly parallel to the orientation of fibrous materials within MSW specimens (Bray *et al.*, 2009; Zekkos *et al.*, 2010). For the conventional triaxial compression test results, a specific strain was normally used as failure criterion to calculate the MSW strength parameters (Caicedo *et al.*, 2002; Machado *et al.*, 2002; Vilar and Carvaho

*Assistant professor, College of Civil Engineering and Architecture, China Three Gorges University, Yichang 443002, China (Corresponding Author, E-mail: hellolixiulei@163.com)
**Professor, Key Laboratory of Ministry and Education for Geomechanics and Embankment Engineering, Hohai University, Nanjing, 210098, China (E-mail: soft-ground@hhu.edu.cn)

2004; Zhan *et al.*, 2008; Karimpour-Fard *et al.*, 2011). Zekkos *et al.* (2012) reported a method for determining MSW strength parameters that MSW specimens were assumed failure at an axial strain of 5% from at rest stress state conditions (Coefficient of static lateral earth pressure $K_0 = 0.3$).

The effects of waste composition, unit weight, loading rate, fibrous content and moisture content on the stress-strain responses have been investigated by some authors (Zhan *et al.*, 2008; Reddy *et al.*, 2011; Nayebi *et al.*, 2011; Karimpour-Fard *et al.*, 2011; Zekkos *et al.*, 2012). The stress path is also a main influence on mechanical properties of MSW (Zekkos *et al.*, 2012). To the best knowledge of the authors, however, few studies have been reported on the effect of stress path on stress-stain responses of MSW. Loading and unloading conditions are both likely to occur in landfills with filling, degradation and settlement. Both conventional triaxial compression test and direct shear test are difficult to reflect the stress-strain of MSW fully. In this paper, it is hoped that an understanding of the mechanical responses of MSW is improved through stress path tests by using a triaxial apparatus. Finally, a new method is proposed for determining the shear strength parameters of MSW.

2. Material, Equipment and Testing Program

2.1 Composition of MSW

In this paper, the MSW components were determined according to the waste collected from a sanitary landfill located in the outskirts of Yancheng city, China. The waste contained paper, wood, thin plastics sheets, textile, glass, stone and paste (including soil-like and organic mater). Fig. 1 shows the percentage mass of various components of the waste. Fig. 1 also shows a comparison between the composition of MSW used in this study with the composition of MSW used in other published studies. The paste was composed of 24% of organic mater and 28% of soils within MSW. The sheet-like materials such as paper, plastic and textile are all classified to a group of fibrous material that is regarded as a reinforcing material in MSW. The plastic and textile can withstand a great tensile strength, but the tensile strength of paper is relative small after soaking.

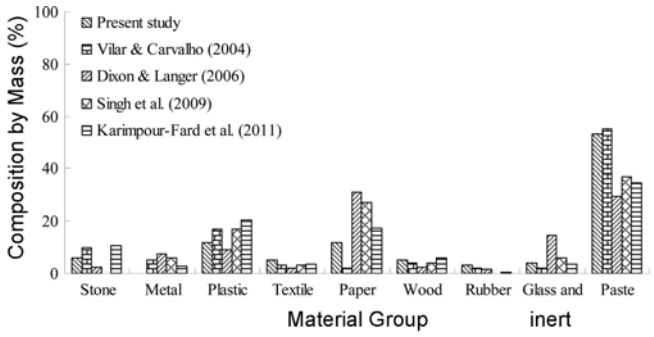

Fig. 1. Composition of the MSW Used in This Study in Comparison to MSW Used in Other Studies

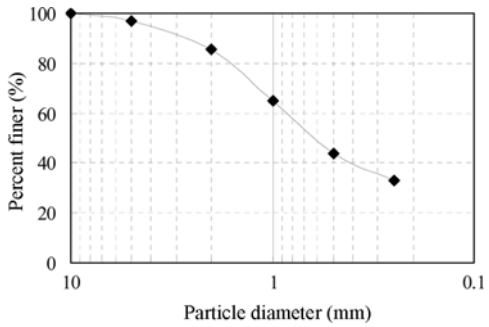

Fig. 2. Particle Diameter Distribution Curves of MSW

2.2 Specimen Preparation

Zhan *et al.* (2008) reported that the dry densities of MSW mainly fall in the range of 0.4 to 1.0 g/cm^3 and the void ratio is from 1.24 to 3.76. In the statistics on the dry density and void ratio of MSW reported by Tu and Qian (2008), it is found that the dry density of MSW ranged from 0.55 to 0.96 g/cm^3 and the void ratio ranged from 1.00 to 3.70. To assure all the MSW specimens with the same initial state (for instance void ratio, composition, density and dimension, etc.), artificial prepared reconstituted samples were used in this study rather than undisturbed samples. The MSW specimens had a diameter of 40 mm, height of 86 mm, dry density of 0.70 g/cm^3, initial void ratio of 2.0 and initial moisture content of 50%. The average grain size distribution of the MSW specimens is depicted in Fig. 2. In this curve, fibrous materials are not included. As can be seen, the largest particle diameter is about 5 mm, with about 65% being finer than 1.0 mm. To avoid the influence of particle size on stress-strain responses of MSW, the length of fibrous materials should be consistent as far as possible. According to the studies on fiber reinforced clay and sand soils by Ghazavi and Roustaie (2010), Ple and Le (2012) and Jamei *et al.* (2013), the fiber length should be less than 1/3 of the specimen diameter in this study. The waste paper was cut into pieces with specified length and width by a shredder. The length of plastic and textile could be controlled by the methods of manual cutting and measurement.

The methodology described in the Chinese Standard for soil test method (GB/T 50123-1999) was used for MSW specimen preparation. According to the known dry density and volume of a MSW specimen, the weight of a MSW specimen could be calculated. Each component within a MSW specimen could also be determined and weighted based on the percentage mass distribution of various components as presented in Fig. 1. All the MSW components were carefully mixed manually to get a homogeneous mixture. In the meantime, the required amount of water was added to the mixture increasingly. The mixture was divided into five parts. Each part was poured in the split mold and was compacted using a metal hammer until the desired height was reached. This procedure was repeated five times to obtain a fully compacted MSW specimen.

Firstly, the prepared MSW specimens were saturated by vacuum

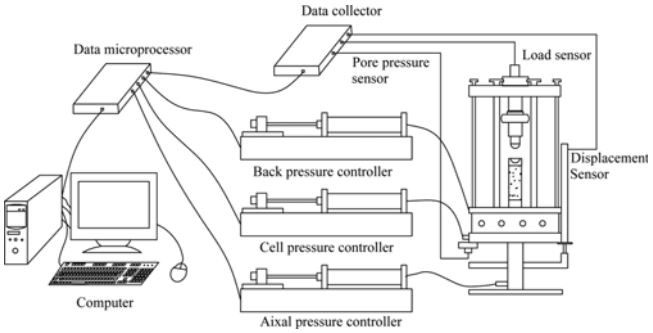

Fig. 3. The Schematic Diagram of the Triaxial Test Apparatus

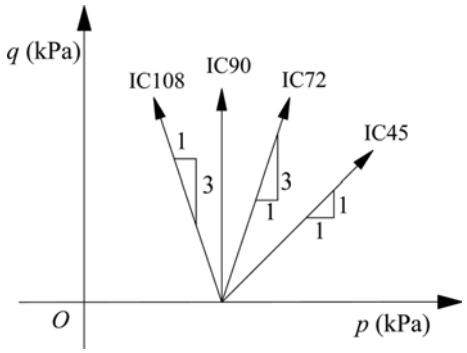

Fig. 4. Test Program for MSW Specimens Under Isotropic Consolidation

saturation method in accordance with the Chinese Standard for soil test method (GB/T 50123-1999). Secondly, the saturated specimens were installed into pressure chamber. Thirdly, the saturation techniques was used with upward flow (using an effective confining pressure of 10 kPa) until the stationary flow was reached. Finally, the specimen was saturated again by using back-pressure saturation techniques which is the same as what Karimpour-Fard *et al.* (2011) reported. A minimum value of saturation coefficient $B = 0.9$ was adopted for considering the MSW specimens in saturation state. After saturation, the MSW specimen was consolidated until the volume change rate was negligible. The triaxial tests were carried out at a shearing rate of 0.02 mm/min based on the Chinese Standard for soil test method (GB/T 50123-1999). The maximum axial displacement is 27 mm for the triaxial device.

2.3 Triaxial Device

An advanced stress path triaxial test apparatus was used to evaluate the mechanical behavior of MSW. Fig. 3 shows the schematic diagram of the apparatus. The equipment has three different systems which are pressure chamber, control system and a data measuring system. The control system includes back pressure controller, cell pressure controller and axial pressure controller. The first controller is connected with MSW specimen to measure the changes in the volume of water inside the specimen. The second controller is connected with the pressure chamber to control the confining stress on MSW specimen by the medium of water. The third controller enables the performance of the axial stress on the MSW specimen installed in the pressure chamber. The data measurement system consists of the following parts, data sensors (e.g., axial stress sensor, axial displacement sensor and pore pressure sensor), data collector, data microprocessor and computer. The data is automatically collected and displayed on the computer screen. The stress path tests could be carried out by this triaxial test apparatus with a loading capacity of 1700 kPa in confining stress and 7 kN in axial strength. The control accuracy of volume measurement is 1 mm^3. The accuracy of the measured pressure is 1 Pa. The equipment and software meets the requirements of this study.

2.4 Test Schedule

All MSW specimens were tested by triaxial test under isotropic consolidated drained conditions after saturation. Four stress paths in *p*-*q* space were performed in Fig. 4, including IC45, IC72, IC90 and IC108 tests. In this study, the purpose of all performed tests was to investigate the effect of stress path on stress-strain behavior and strength properties of MSW. The above four stress paths all belong to compression test. The confining stress increment $\Delta\sigma_3$ is greater than 0 (ie. $\Delta\sigma_3 > 0$) for IC45 test, $\Delta\sigma_3 = 0$ for IC72 test, $\Delta\sigma_3 < 0$ for IC90 and IC108 tests. The MSW specimens were tested under several isotropic consolidation pressures of 100, 200, 300 and 400 kPa for each stress path test, and 500 kPa for IC72 test. For the example of IC90 path, 'IC' represents isotropic consolidation and '90' represents the angle θ (positive counterclockwise herein) between the p'-axis direction and present stress path direction in p'-q space. Other relevant information is shown in Table 1. Under axisymmetric conditions, the mean normal effective stress p' and the deviator stress q are defined as

$$p' = (\sigma_1' + 2\sigma_3')/3 \; ; \; q = \sigma_1' - \sigma_3' \tag{1}$$

where, σ_1' and σ_3' are axial effective stress and radial effective stress, respectively.

Shear modulus G is defined as

$$G = dq/3d\varepsilon_s \tag{2}$$

During tests, the drainage volume within the back-pressure chamber is the volume change of the MSW specimens. Axial displacement is measured by a displacement sensor outside the pressure chamber. The radial strain ε_r and shear strain ε_s could be calculated from Eq. (3) (Karimpour-Fard *et al.*, 2011):

Table 1. Description of Four Axial Compression Stress Path Tests

Label	θ(°)	Description	Remark
IC45	45	Anisotropic loading	$\Delta\sigma_1/\Delta\sigma_3 = 2.5$; $\Delta\sigma_3 > 0$
IC72	72	Conventional triaxial compression	$\Delta\sigma_1 > 0$; $\Delta\sigma_3 = 0$
IC90	90	Constant mean normal compression	$\Delta\sigma_1/\Delta\sigma_3 = -2.0$; $\Delta\sigma_3 < 0$
IC108	108	Reduced Anisotropic compression	$\Delta\sigma_1/\Delta\sigma_3 = -0.5$; $\Delta\sigma_3 < 0$

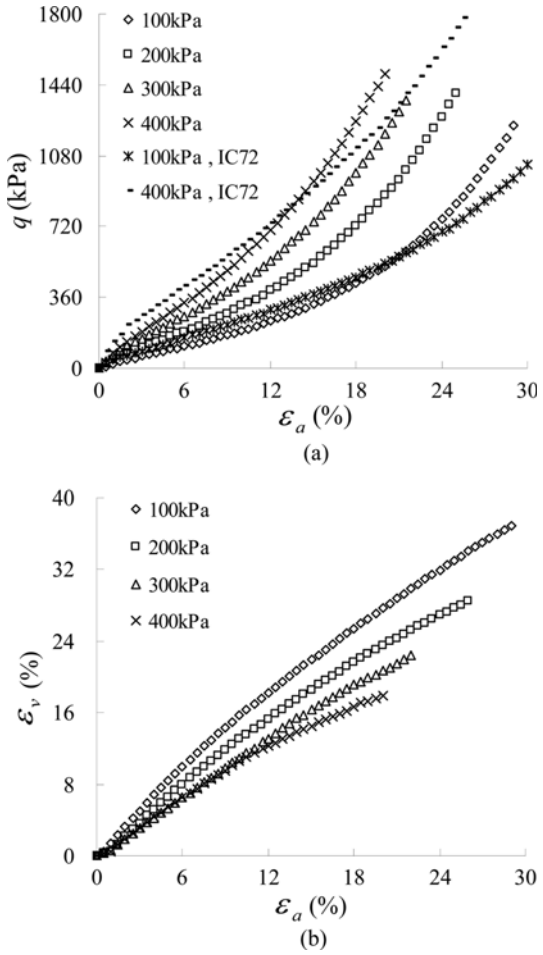

Fig. 5. Triaxial Test Results of MSW in IC45 Test: (a) q-ε_a Curves in IC45 Test in Comparison with IC72 Test, (b) ε_v–ε_a curves in IC45 test

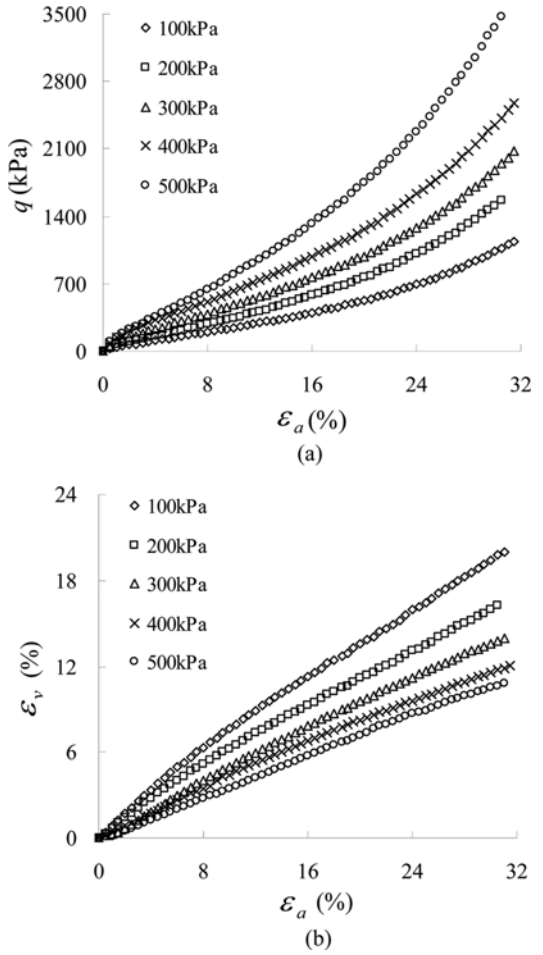

Fig. 6. Triaxial Test Results of MSW in IC72 Test: (a) q-ε_a Curves in IC72 Test (Conventional Triaxial Compression Test), (b) ε_v–ε_a Curves in IC72 Test

$$\varepsilon_r = 1 - \sqrt{\frac{1-\varepsilon_v}{1-\varepsilon_a}};\ \varepsilon_s = \frac{2}{3}(\varepsilon_a - \varepsilon_r) \tag{3}$$

where ε_a and ε_v are axial strain and volumetric strain, respectively.

3. Triaxial Test Results and Discussion

Figure 5, Fig. 6, Fig. 7 and Fig. 8 present the stress-strain responses of MSW specimens in IC45, IC72, IC90 and IC108 tests, respectively. It is observed that both stress path and pre-consolidation pressure have significant effect on the stress-strain responses of MSW. For the same stress path, the shear strength of MSW specimen is increased with the increase of pre-consolidation pressure. All the MSW specimens have the same stress state, void ratio and dimension after consolidation under the same pre-consolidation pressure conditions. When the pre-consolidation pressures and axial strains are respectively equal, the order of void ratios, volumetric strains and diameters from smallest to largest is IC45, IC72, IC90 and IC108 tests as shown in Table 2 and Fig. 9. During triaxial tests, the confining stress increment $\Delta\sigma_3$ and the mean normal effective stress increment $\Delta p'$ are both larger than zero for IC45 test, $\Delta\sigma_3 = 0$ and $\Delta p' > 0$ for IC72 test, $\Delta\sigma_3 < 0$ and $\Delta p' = 0$ for IC90 test, $\Delta\sigma_3 < 0$ and $\Delta p' < 0$ for IC108 test. The volume changes of MSW specimen is positively correlated with the mean normal effective stress p' during testing. Under the same pre-consolidation pressure conditions, therefore, the volumetric strain of MSW specimens obtained from IC45, IC72, IC90 and IC108 tests is decreased one by one at the same axial strain. Under the same pre-consolidation pressure, Fig. 9 presents the illustrations of MSW specimens for different stress path at the same axial strain. The diameter of specimen is reduced in IC45 test; the diameter of specimen is increased in IC72, IC90 and IC108 paths.

3.1 The Stress-strain Responses of MSW Specimens for Compression Stress Path of $\Delta\sigma_3' \geq 0$

The stress-strain responses of MSW specimens in IC 45 and IC72 tests are shown in Fig. 5 and Fig. 6. From Fig. 5(a), all the stress-strain curves in IC45 test exhibit a linear growth section initially followed by an upward curvature at large strains (i.e. $\varepsilon_a > 10\%$). As shown in Fig. 6(a), for IC72 test, all the stress-

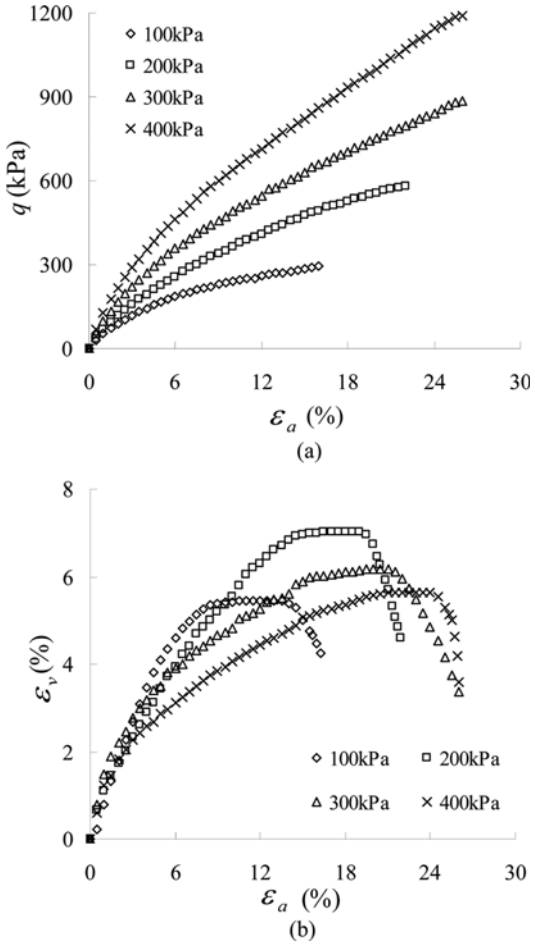

Fig. 7. Triaxial Test Results of MSW in IC90 Test: (a) q-ε_a Curves in IC90 Test, (b) ε_v–ε_a Curves in IC90 Test

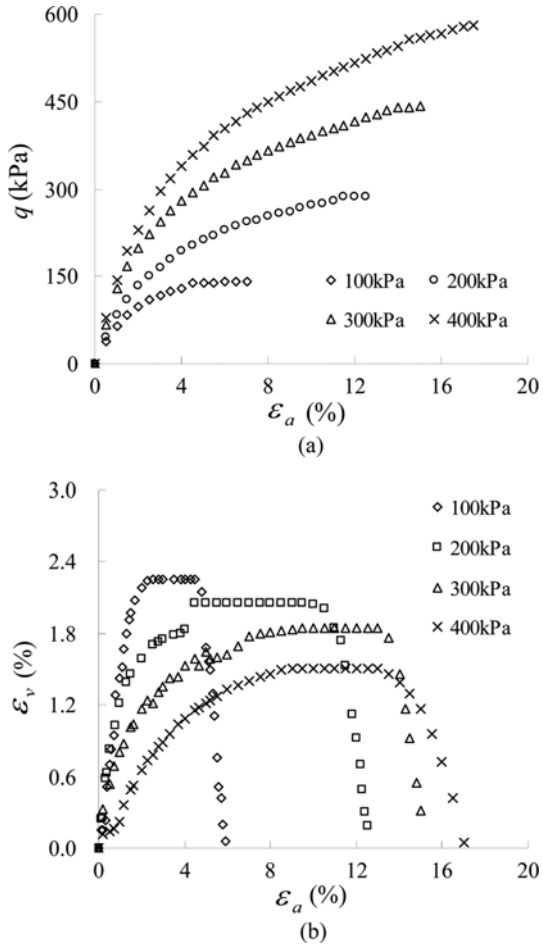

Fig. 8. Triaxial Test Results of MSW in IC108 Test: (a) q-ε_a Curves in IC108 Test, (b) ε_v–ε_a Curves in IC108 Test

strain curves have the same shape, with a downward bending at small strains (i.e. $\varepsilon_a < 5\%$) followed by a linear growth section and then an upward curvature (i.e. $\varepsilon_a > 20\%$). A peak or an asymptotic value is not observed in MSW stress-strain curves for IC45 and IC72 tests. Under the confining stress of 100 kPa conditions, for the example of IC72 tests, the stress-strain curves of MSW specimens with different dimensions are presented in Fig. 10. In contrast to large MSW specimen, as can be seen from Fig. 10, it is found that the small specimen exhibit a larger shear strength at the same axial strain. However, all the stress-strain curves of MSW specimens have similar shape. Therefore, it is viable to study the mechanical properties of MSW by using the preparation MSW specimen in this study.

Michalowski and Cernak (2002) performed a series of monotonic triaxial compression tests on sand specimens reinforced with polyamide fiber. An upward curvature was also observed at large strains in stress-strain responses. Sand reinforced with vertically oriented fibers did not increase in shear strength. An analogy can be made for MSW, MSW is composed of soil-like materials with reinforced fibrous materials. The orientation of fibrous materials within MSW is generally horizontal (Zekkos *et al.*, 2005). It is suggested that the upward curvature observed in IC45 and IC72 tests is attributable to the progressive contribution of fibrous materials when the shear surface cut across the long axis of the fibrous materials. For IC45 and IC72 tests, it can be added that, the lateral deformation of specimen is restrained during tests because of $\Delta\sigma_3 \geq 0$ and the observed upward curvature in triaxial testing is progressive re-structuring of the specimen. As vertical load increases, the original structure of the specimens with horizontal oriented fibrous becomes more pronounced, the contact between soil-like materials and fibrous materials become more closely, and the tensile strength of fibers within MSW specimens play more fully, increasing further the strength of MSW in triaxial compression.

When the pre-consolidation pressures are the same, the initial section of stress-strain curves obtained by the IC45 test is located below the IC72 test results. It can be attributed to the increase of σ_3 which caused the porosity within MSW specimen to reduce faster for IC45 test. Thus, a smaller deviator stress is needed in IC45 test comparing with IC72 test at the same axial strain. However, the deviator stresses obtained in IC45 test are larger than that in the IC72 test at large strains ($\varepsilon_a > 15\%$). Compared with IC72 test, as the vertical and horizontal stress increase, the void ratios of MSW specimen become smaller in IC45 test

Table 2. The Void Ratios of MSW Specimens

Stress path	label	Pre-consolidation confining pressure (kPa)				
		100	200	300	400	500
IC45	e_1	1.629	1.418	1.243	1.093	
	e_{20}	0.902	0.85	0.78	0.717	
	e_0–e_1	0.371	0.582	0.757	0.907	
	e_1–e_{20}	0.727	0.568	0.463	0.376	
IC72	e_1	1.645	1.398	1.206	1.086	1.002
	e_{20}	1.285	1.13	0.996	0.914	0.858
	e_{30}	1.131	1.015	0.906	0.844	0.792
	e_0–e_1	0.355	0.602	0.794	0.914	0.998
	e_1–e_{20}	0.36	0.268	0.21	0.172	0.144
	e_1–e_{30}	0.514	0.383	0.3	0.242	0.210
IC90	e_1	1.636	1.44	1.254	1.118	
	e_f	1.496	1.27	1.114	1.005	
	e_0–e_1	0.364	0.56	0.746	0.882	
	e_1–e_f	0.14	0.17	0.14	0.113	
IC108	e_1	1.61	1.399	1.222	1.109	
	e_f	1.551	1.351	1.18	1.078	
	e_0–e_1	0.39	0.601	0.778	0.891	
	e_1–e_f	0.059	0.048	0.042	0.031	

Note: The initial void ratio e_0 of MSW specimen is 2.0; e_1 represents the void ratio after consolidation; e_{20}, e_{30} and e_f represent the void ratio at the axial strain of 20%, 30% and at the end of the tests, respectively; e_0–e_1 represent the reduction of void ratio after consolidation; e_1–e_{20}, e_1–e_{30} and e_1–e_f represent the reduction of void ratio at axial strain of 20%, 30% and at the end of the tests from after consolidation, respectively.

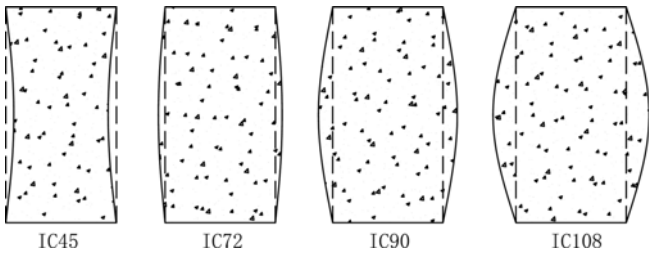

Fig. 9. The Illustrations of MSW Specimens for Different Stress Path at the Same Axial Strain

because of $\Delta\sigma_3 > 0$ (see Table 2). It indicates that the contact between soil-like materials and fibrous materials becomes more closely, resulting in more pronounced fibrous reinforcement.

As shown in Fig. 5(b) and Fig. 6(b), another interesting feature is the decrease in volume as the consolidation pressure increases, which has been observed by some authors such as Machado *et al.* (2002) and Karmpour-Fard *et al.* (2011). The initial void ratio of MSW specimen is 2.0. The void ratios of MSW specimen are shown in Table 2. Under pre-consolidation pressure 500 kPa, for the example of IC72 test, the reduction of void ratio is 0.998 after consolidation which is the largest, but the reduction of void ratio is only 0.21 at the axial strain of 30% from after consolidation which is the smallest. In other words, a larger pre-consolidation pressure causes a larger reduction of void ratio during consolidation and a smaller reduction of void ratio during test. Therefore, the above results suggest that a large pre-consolidation pressure results in a small volumetric strain during the test.

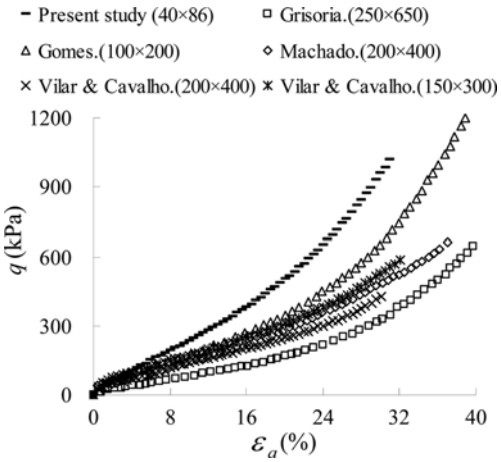

Fig. 10. For IC72 Test, the Comparison of q-ε_a Curves for Different MSW Specimens with Different Dimensions Under Confining Stress of 100 kPa

3.2 The Stress-strain Responses of MSW Specimens for Compression Stress Path of $\Delta\sigma_3 < 0$

The stress-strain responses of MSW specimens in IC90 and IC108 tests are shown in Fig. 7 and Fig. 8. From Fig. 7(a) and Fig. 8(a), the stress-strain responses of all MSW specimens exhibit a rapidly increasing section initially followed by a slowly increasing section at large strains without upward curvature like that in IC45 and IC72 tests. Because of the reduction of confining stress in IC90 and IC108 tests, the lateral constraint of MSW specimens are gradually weakened during testing. As can be seen from Fig. 9 and Table 2, the void ratios and radial deformation of MSW specimens in IC90 and IC108 tests are much larger than that in IC45 and IC72 test at the same axial strain. It indicates that the contact between fibrous materials and other soil-like particles within MSW specimens is not close enough to ensure the tensile strength and reinforcement of fibrous to be developed fully. The axial strain-volumetric strain (ε_a–ε_v) relations of MSW specimens in IC90 and IC108 tests are presented in Fig. 7(b) and Fig. 8(b). All the ε_a–ε_v curves have a similar shape, with a rapid increase section initially followed by a horizontal section and then a rapid decrease section as confining pressure gets close to zero. Although $\Delta p'$ is negative in IC108 test, the volumetric strain is positive, which indicates that the increase of q results in development of the volumetric strain.

The influence of stress history on stress-strain response of MSW specimen is investigated in this paper. The test program on MSW specimen is shown in Fig. 11(a). Firstly, the prepared MSW specimen was consolidated under a confining pressure of 300 kPa. After consolidation, the specimen was tested on IC108 test (loading stage 1). When the confining pressure was reduced to zero, the vertical load was increased continuously under zero confining stress (loading stage 2). The stress-strain response of specimen is presented in Fig. 11(b). For the loading stage 1, the MSW stress-strain relation is in form of a hyperbolic shape with

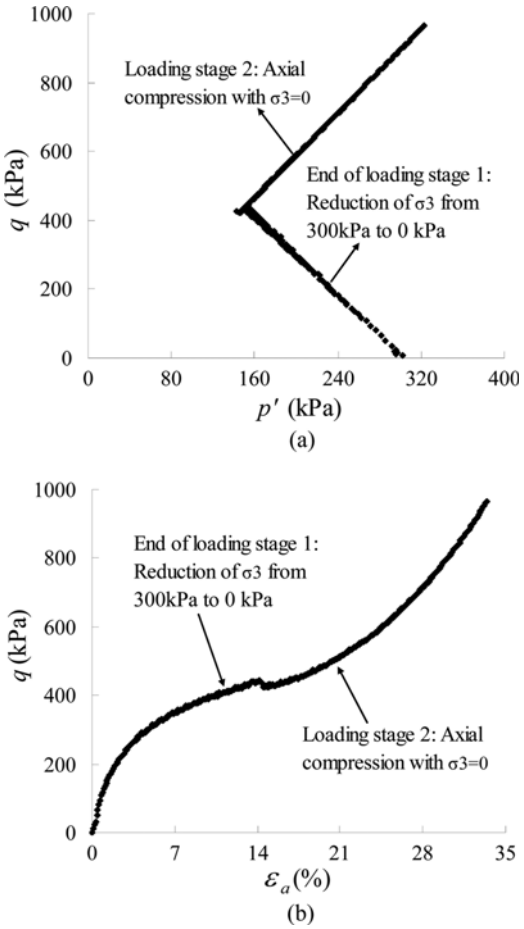

Fig. 11. Stress Paths and Stress-strain Responses for Triaxial Compression Unloading and the Subsequent Unconfined Compression Test: (a) Stress Path, (b) q-ε_a Curves

no dilatancy. For the loading stage 2, although σ_3 was zero, the specimen stress-strain response also exhibits an upward curvature without reaching peak conditions. The above test results indicate that MSW is a strain hardening material. Much like soils, the stress-strain response of MSW is affected significantly by previous stress history. MSW specimen that has been consolidated at a higher confining pressure and subsequently unloaded has a higher strength at lower confining stress than the strength of MSW specimen at the same confining stress that has not previously experienced the higher confining stress. The fibrous nature and interlocking structure among particles within MSW when pre-loaded likely makes the effect of stress history more pronounced for MSW, which also illustrates the upward curvature in stress-strain curve for MSW specimen without confining stress. These test results also provide a possible explanation for the field observations of vertical waste slope being stable for a period of months to years (Eid *et al.*, 2000).

3.3 The Effect of Stress Paths on MSW Shear Modulus

For IC45, IC72, IC90 and IC108 tests, the relationships between tangential shear modulus G of MSW and axial strain ε_a under consolidation pressure of 100 kPa were shown in Fig. 12. For IC45 and IC72 tests, at large strains, the shear modulus G of MSW increases with increasing strain instead of reduction. However, for the clay and sand soils, the decreasing trend in the shear modulus G with increasing strain for different stress path tests has been reported by Cho and Finno (2010) and Oztoprak and Bolton (2013). The above obvious differences between MSW and soils could be attributed to fibrous reinforcement in MSW specimens under vertical loading. As a result of the fibrous reinforcement, the deformation of MSW is relative smaller than that of soils at the same increment of deviator stress Δq in IC72 tests at the large strains. The G-ε_a curve obtained by IC45 test is located below the curve in IC72 test at small strains, which is reverse at large strains ($\varepsilon_a > 24\%$). For IC45 and IC72 tests, the conditions of G-ε_a relations are similar with the q-ε_a relations. For IC72 test, the reduction section and nonlinear increasing section in G-ε_a curve are corresponding to the downward curvature and upward curvature in q-ε_a curve, respectively. For IC 45 test, the linear slowly growth section and rapidly growth section are corresponding to the linear increasing section and upward curvature in q-ε_a curve, respectively. Therefore, the G-ε_a responses confirm the conditions in q-ε_a responses.

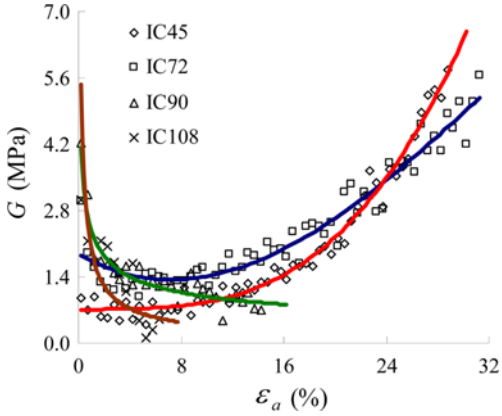

Fig. 12. The Relationships between Shear Modulus of MSW and Axial Strain for Different Stress Paths Tests with Isotropic Consolidation Pressure σ_3 = 100 kPa

For IC90 and IC108 path tests, the MSW shear modulus G is generally in the form of exponential decay with increase of ε_a, which is similar with clay and sand soils. However, the decay rate of G in IC108 test is much larger than that in IC90 test, which confirms the conditions in q-ε_a responses.

3.4 Method for Determining MSW Strength Parameters

3.4.1 Strength Parameters of MSW in IC72 Tests

As observed from Fig. 5(a) and Fig. 6(a), each q-ε_a curve of MSW specimen has the similar shape in IC45 and IC72 tests, with a linear increasing section followed by an upward curvature. The transitional point between linear increasing section and upward curvature in q-ε_a curves is defined as hardening point. Before the hardening point, the shear strength of MSW depends

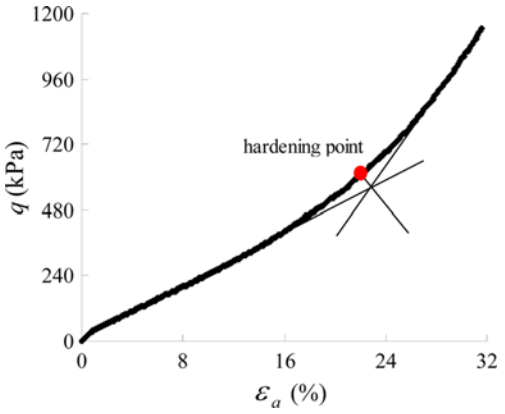

Fig. 13. The Determination of Hardening Point in Stress-strain Curve of MSW in IC45 and IC72 Tests

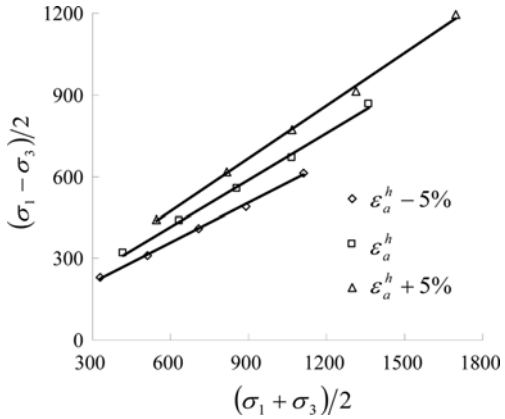

Fig. 14. Shear Strength Envelopes of MSW for Different Strains in IC72 Test

Table 3. The Axial Strain and Deviator Stress at Hardening Points in q-ε_a Curves in IC45 and IC72 Path Tests Under Different Consolidation Pressure Conditions

Stress path	Label	Pre-consolidation pressure (kPa)				
		100	200	300	400	500
IC45	ε_a^h (%)	19.2	16.3	14.1	12.8	-
	q (kPa)	481.6	645.0	679.0	719.8	-
IC72	ε_a^h (%)	22.8	22.0	21.8	21.4	19.9
	q (kPa)	640.5	872.7	1109.4	1337.6	1729.5

Note: ε_a^h represents the axial stain at hardening point in stress-strain curves for IC72 and IC 45 tests.

Table 4. Stress Strength Parameters of MSW for Different Stress Path Tests

Stress path	Axial strain (%)	Shear strength envelopes (s–t diagram) (kPa)	R^2	c (kPa)	φ (°)
IC72	ε_a^h–5%	$t = 0.505s + 49.085$	0.997	56.9	30.3
	ε_a^h	$t = 0.586s + 57.814$	0.997	71.3	35.9
	ε_a^h+5%	$t = 0.657s + 70.891$	0.997	94.0	41.1
IC90	ε_a^f	$t = 0.527s + 23.414$	0.998	26.8	32.6
IC108	ε_a^f	$t = 0.498s + 23.660$	0.997	18.6	35.5

Note: $t = (\sigma_1 - \sigma_3)/2$, $s = (\sigma_1 + \sigma_3)/2$; ε_a^h represents the axial stain at hardening point in stress-strain curves for IC72 tests; ε_a^f represents the axial stain at failure point in stress-strain curves for IC90 and IC 108 tests.

on the friction effect among particles within MSW. After the hardening point, the fibrous reinforcement plays a key role in the shear strength of MSW. The hardening point of MSW is defined as the intersection of stress-strain curve and the angle bisector between rectilinear extrapolation of straight-line increase section and upward curvature. Fig. 13 presents the determination of hardening point in stress-strain curves for MSW in IC45 and IC1C72 tests. The axial strain and deviator stress at hardening points in IC45 and IC72 test under different consolidation pressure conditions are shown in Table 3.

As observed in Table 3, the axial strains at hardening points are from 12.8% to 19.2% for IC45 test and from 19.9% to 22.8% for IC72 test. The axial strains of hardening points are not consistent under different pre-consolidation pressures. For instance IC72 test, the fibrous reinforcement is more pronounced under pre-consolidation pressure of 500 kPa than that under other smaller pre-consolidation pressure at the same axial strain of 20%. Therefore, using a strain as failure criterion is inappropriate to calculate the MSW shear strength parameters.

Zekkos *et al.* (2012) proposed an approach to define the shear strength parameters of MSW based on the results in conventional triaxial test (i.e., IC72 test). It is assumed that the MSW specimen fails at an axial strain of 5% from at-rest stress state condition ($K_0 = 0.3$). For the results of MSW specimens in IC72 test under the consolidation pressures of 100, 200, 300, 400 and 500 kPa, according to the above method reported by Zekkos *et al.* (2012), the corresponding axial strains are separately 18.5, 23.3, 24.7, 25.6 and 24.5% when specimens fail. As shown in Table 3, for the two isotropic consolidated specimens under confining pressures of 100 and 500 kPa, the fibrous reinforcement has not been reflected obviously at 18.5% of axial strain in the former specimen; and the fibrous reinforcement is very pronounced at 24.5% of axial strain in the latter specimen. Thus, using $K_0 = 0.3$ and $\varepsilon_a = 5\%$ as failure criterion to define the MSW strength is not appropriate.

The axial stress σ_1 and confining stress σ_3 are both increasing during IC45 test. When the landfill fails, the axial stress and confining stress are unlikely to increase at the same time for the MSW near failure surface. Thus, the strength parameters of MSW in IC45 test are not considered in this study. Based on the results in IC72 test in this paper, the strength of MSW is calculated by using the stress state at hardening point in q-ε_a curve as failure criterion. In other words, it is assumed that the MSW specimens fail at the hardening points. This is different from the approaches proposed by Grisolia *et al.* (1995); Machado *et al.* (2002); Karimpour-Fard *et al.* (2011) and Zekkos *et al.* (2012). Using the hardening point as a reference point, the MSW strength parameters are calculated at the axial strains of ε_a–5%, ε_a and ε_a+5%. The shear envelops of MSW for IC72 test are shown in Fig. 14. Table 4 presents the MSW strength parameters. The cohesions are respective 56.9, 71.3 and 94.0 kPa and the

Table 5. List of Literatures Reported Shear Strength Parameters in Conventional triaxial Compression Tests

References	Size (mm)	Specimen information	Axial strain (%)	c' (kPa)	ϕ' (°)
Grisolia *et al.* (1995)	250×600	The unit weight of MSW specimen was relatively low (CUTX)	15	3	20
Caicedo *et al.* (2002)	300×600	1 year old unshredded MSW (CDTX)	15	14	45
Machado *et al.* (2002)	150×300	15 years old degraded MSW; (CDTX)	20	71	27
	200×400			58	21
Vilar and Carvaho (2004)	150×300	15 years old degraded MSW (CDTX)	20	60.4	23.2
	200×400			52.8	20.7
Zhan *et al.* (2008)	100×200	1.7 to 11 years old degraded MSW (CDTX)	10	0-23.3	9.9-26
Reddy *et al.* (2009)	50×100	Fresh to degraded synthetic MSW (CUTX)	15	38	16
Singh *et al.* (2010)	210×450	Intact and recompacted specimens of MSW (CUTX)	-	0-8.4	35-47
Reddy *et al.* (2011)	50×100	Fresh to degraded synthetic MSW (CUTX)	15	18-56	6-11
Karimpour-Fard *et al.* (2011)	200×350	About 30% of MSW particles are larger than 50 mm; the fiber content is 25% (CDTX)	15	34	18
			20	46	20

Note: CUTX represents consolidation undrained conventional triaxial compression tests; CDTX represents consolidation drained convention triaxial compression tests.

friction angles are respective 30.3°, 35.9° and 41.1° at the axial strains of ε_a^h–5%, ε_a^h and ε_a^h+5%. It is found that the strength parameters are increasing with increasing strains. The larger strength parameters of MSW at large strain level can be in part credited to the more pronounced fibrous reinforcement at large strains. Using the hardening point as failure criterion to evaluate the shear strength parameters of MSW, the most fibrous reinforcement can be regarded as security reserve of landfill stable. Comparing with the test results reported in other studies (see Table 5), the higher shear strength of MSW in this study can be in part contributed by the smaller dimension of MSW specimen used in this study and to the high content of crushed stones and soils within MSW specimens.

Mohr-Coulomb strength envelope is expressed as follows:

$$\sigma_1 = 2c\tan\left(\frac{\varphi}{2}+45^\circ\right) + \sigma_3\tan^2\left(\frac{\varphi}{2}+45^\circ\right) \quad (4)$$

where, c is the cohesion intercept; φ is the friction angle. In conventional triaxial compression tests (i.e., IC72 test), as shown in Fig. 15, the failure surface is roughly at an angle of 45°+φ/2 degrees to the horizontal plan that coincides with the fibrous materials orientation in the statically compacted MSW. For a friction angle of 30-40°, the failure surface is expected to be at angle of 60-65 degrees to the horizontal plan. The stress-strain curves of MSW are normally in the form of hyperbolic shape in direct shear tests. Based on the direct shear test results (Athanasopoulos *et al.*, 2008), the MSW specimen with an angle of about 60° between horizontal failure surface and fibrous materials orientation exhibits the strongest response and upward curvature in stress-strain curves that is similar with the results in conventional triaxial compression tests. Thus, the shear strength in convention triaxial compression tests is higher than that in direct shear tests, which was found by Zekkos (2005) through the comparison of the test results from the above two test types.

3.4.2 Strength Parameters of MSW in IC 90 and IC108 Tests

All the MSW specimens exhibit some strain hardening from Fig. 7(a) and Fig. 8(a), but the upward curvature like that

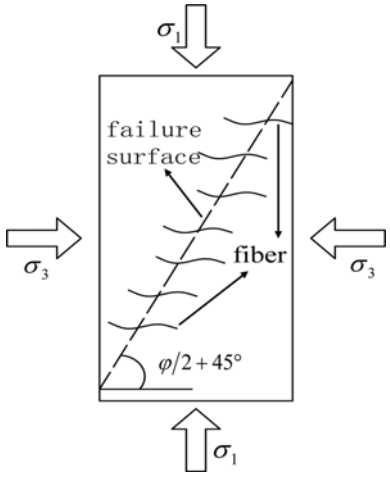

Fig. 15. The Diagram of Triaxial Compression Tests

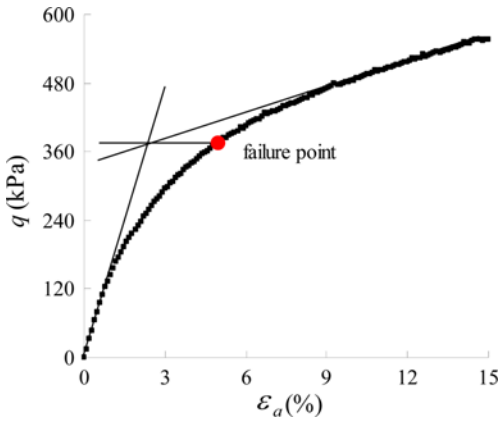

Fig. 16. The Determination of Failure Point in Stress-strain Curve of MSW in IC90 and IC108 Tests

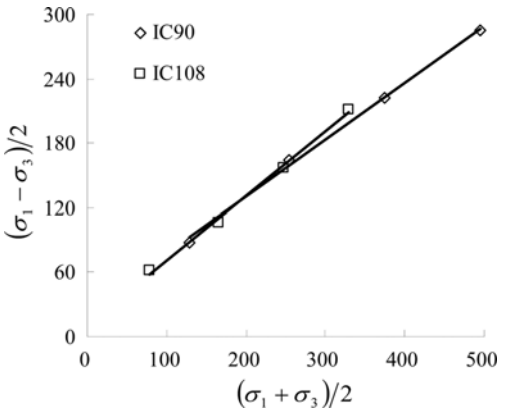

Fig. 17. Shear Strength Envelopes of MSW in IC90 and IC108 Tests

obtained in IC72 and IC45 tests are not observed in stress-strain curves for IC90 and IC108 tests. There is no hardening point in q-ε_a curves of MSW specimen in IC90 and IC108 tests. Therefore, the failure criterion used in IC90 and IC108 tests is not consistent with IC72 test to determine the strength parameters. The failure point of MSW in stress-strain curve is defined as the intersection point between the stress-strain curve and the horizontal line which is through the intersection point between the tangent of the rapidly increasing section and the tangent of the slowly increasing section. Fig. 16 presents the determination of failure point for MSW in IC90 and IC108 tests. The strength of MSW is calculated by using the stress state at failure point on the basis of the results in IC90 and IC108 tests. For the above two tests, the shear strength envelops and strength parameters of MSW are shown in Fig. 17 and Table 4, respectively. As shown in Table 4, the friction angles of MSW are similar for different stress path tests. However, the cohesions of MSW in IC90 and IC108 tests are separately 26.8 and 18.6 kPa which are much smaller than 71.3 kPa obtained in IC72 test. The stress path has a little effect on the friction angle of MSW, but has a significant effect on the cohesion of MSW. Due to the decrease of confining stress, the fibrous reinforcement within MSW specimen is less pronounced in IC90 and IC108 tests relative to IC72 test. As a result, the fibrous reinforcement is able to improve the cohesion of MSW.

4. Conclusions

The stress-strain responses, stiffness and shear strength parameters of a reconstituted MSW have been investigated by four triaxial compression tests under isotropic consolidated drained conditions. The stress path test results of the MSW are important to comprehensively understand the mechanical properties of MSW, which is a supplement for direct shear test and conventional triaxial compression test. For different stress path tests, new methods for determining shear strength parameters of MSW were proposed in this study. The stress-strain behavior of MSW is closely related to the deformation and stability of Landfills. Based on the tests results of MSW presented herein, the following main conclusions can be drawn:

1. The stress path has a significant effect on the stress-strain responses of MSW. The shear strength of MSW is increasing as the pre-consolidation confining pressure increases. For the compression stress path of $\Delta\sigma_3 \geq 0$, all the stress-strain curves of MSW exhibit a linear increase section followed by an upward curvature. For the compression stress path of $\Delta\sigma_3 < 0$, all the stress-strain curves of MSW contain a rapidly increase section and a slowly increase section which are in the form of a hyperbolic shape with no dilatancy. Comparing with IC45 and IC72 tests, the shear strength of MSW is much smaller at large strains in IC90 and IC108 tests because of the reduction in confining stress. Finally, from shear modulus point of view, the stress-strain behavior of MSW is confirmed in different path tests.
2. The void ratios and lateral deformation of MSW specimens before and after triaxial tests are presented in this paper. Under the same pre-consolidation pressure, the volumetric strains of MSW specimens obtained from IC45, IC72, IC90 and IC108 tests are decreased one by one at the same axial strain. The diameter of MSW specimens is reduced in the IC45 test and increased in IC72, IC90 and IC108 tests. For the compression stress path of $\Delta\sigma_3' \geq 0$, the volumetric strains decreases during compression tests with increasing pre-consolidation pressure. Although the $\Delta p'$ is zero in IC90 test and less than zero in IC108 test, the volumetric strains ε_v are positive. It indicates that the development of ε_v can be attributed to the increase of q.
3. For the compression stress path of $\Delta\sigma_3' \geq 0$, the hardening points defined in the q-ε_a curves are used as failure criterion to calculate the shear strength parameters of MSW. For the compression stress path of $\Delta\sigma_3' < 0$, the failure points defined in the q-ε_a curves are also used as failure criterion to calculate the shear strength parameters of MSW. For IC72, IC90 and IC108 tests, the cohesions of MSW are separately 71.3, 26.8 and 18.6 kPa and friction angles of MSW are separately 35.9°, 32.9° and 35.5°. The friction angles are similar for different stress path tests. The cohesions of MSW in compression stress path of $\Delta\sigma_3' < 0$ (IC90 and IC108 tests) are much smaller than that obtained in conventional triaxial compression test (IC72 test). Hence, it is necessary to consider the actual stress state of MSW to analyze the stability of landfill. Due to the reinforcing effects of fibrous materials, the friction angle values obtained by conventional triaxial compression tests are higher than those measured in direct shear tests where shearing occurs parallel to the fibrous orientation.

Consequently, the stress-strain responses and shear strength parameters of MSW are related closely to the stress path. Although the test results are just for the present MSW specimens, the physical and mechanical properties are similar for different MSW materials. In this study, the results of the present MSW are valid reference to understand the mechanical properties of other MSW materials.

Acknowledgements

The authors appreciate the financial support provided by National Natural Science Foundation of China (No. 41172234).

Notation

B : Skempton coefficient
c : Cohesion
e_0 : Initial void ratio of MSW specimen
e_1 : Void ratio of MSW specimen after consolidation
G : Shear modulus
p' : Mean normal effective stress
q : Deviator stress
$\Delta p'$: Increment of mean normal effective stress
Δq : Increment of deviator stress
$\Delta\sigma_3$: Increment of confining stress
ε_a : Axial strain
ε_v : Volumetric strain
ε_r : Radial strain
ε_s : Shear strain;
ε_a^h : The axial stain at hardening point in stress-strain curves for IC72 and IC108 tests
ε_a^f : The axial stain at failure point in stress-strain curves for IC90 and IC 108 tests
φ : Friction angle
σ_1' : Axial effective stress
σ_3' : Confining effective stress

References

Athanasopoulos, G., Grizi, A., Zekkos, D., Founta, P., and Zisimatou, E. (2008). "Municipal solid waste as a reinforced soil: Investigation using synthetic waste." *ASCE-Geoinstitute Geocongress*, pp. 168-175, DOI: 10.1061/40970(309)21.

Bray, J. D., Zekkos, D., Kavazanjian, E. Jr., Athanasopoulos, G. A., and Riemer, M. F. (2009). "Shear strength of municipal solid waste." *Journal of Geotechnical and Geoenvironmental Engineering*, Vol. 135, No. 6, pp. 709-722, DOI: 10.1061/(ASCE)GT.1943-5606.0000063.

Caicedo, B., Yamin, L., Giraldo, E., and Coronado, O. (2002). "Geomechanical properties of municipal solid waste in Dona Juana sanitary landfill." *Proceeding of the 4th International Coongress on Environmental Geotechnics*, Brazil, Vol. 1, pp. 177-182.

Cho, W. J. and Finno, R. J. (2010). "Stress-Strain Responses of Block Samples of Compressible Chicago Glacial Clays." *Journal of Geotechnical and Geoenvironmenal Engineering*, Vol. 136, No. 1, pp. 178-188, DOI: 10.1061/(ASCE) GT.1943-5606.0000186.

Dixon, N. and Jones, D. R. V. (2005). "Engineering properties of municipal solid waste." *Geotextiles and Geomembranes*, Vol. 23, No. 3, pp. 205-233, DOI: 10.1016/j.geotexmem.2004.11.002.

Eid, H. T., Stark, T. D., Evans, W. D., and Sherry, P. E. (2000). "Municipal solid waste slope failure. I: Waste and foundation soil properties." *Journal of Geotechnical and Geoenvironmental Engineering*, Vol. 126, No. 5, pp. 397-407, DOI: 10. 1061/(ASCE) 1090-0241 (2000) 126:5(397).

Gabr, M. A. and Valero, S. N. (1995). "Geotechnical properties of municipal solid waste." *Geotechnical Testing Journal*, Vol. 18, No. 2, pp. 241-251, DOI: 10.1031/(ASTM) 0149-6155(1995)18:2(241).

Gabr, M. A., Hossain, M. S., and Barlaz, M. A. (2007). "Shear strength parameters of municipal solid waste with leachate recirculation." *Journal of Geotechnical and Geoenvironmental Engineering*, Vol. 133, No. 4, pp. 478-484, DOI: 10.1061/(ASCE)1090-0241(2007)133:4(478).

GB/T 50123-1999 (1999). Standard for soil test method. *The national standard of the People's Republic of China*, China planning press, Beijing, China.

Ghazavi, M. and Roustaie, M. (2010). "The influence of freeze-thaw cycles on the unconfined compressive strength of fiber-reinforced clay." *Cold Regions Science and Technology*, Vol. 61, No. 2, pp. 125-131, DOI: 10.1016/j.coldregions.2009.12.005.

Gomes, C., Ernesto, A., and Lopes, M. L. (2002). "Sanitary landfill of Santo Triso-municipal waste physical, chemical and mechanical properties." *Proceeding of the 4th International Coongress on Environmental Geotechnics*, Brazil, Vol. 1, No. 3, pp. 255-261.

Grisolia, M., Napoleoni, Q., and Tangredi, G. (1995). The use of triaxial tests for the mechanical characterization of municipal solid waste. *In proceeding of the 5th International Landfill Symposium*, Sardinia, Vol. 95, No. 2, pp. 761-767.

Hendron, D. M., Fernandez, G., Prommer, P. J., Giroud, J. P., and Orozco, L. F. (1999). "Investigation of the cause of the 27 September 1997 slope failure at the Dona Juana landfill." In *Proceedings Sardinia 1999. 7th International Waste Management and Landfill Symposium*, pp. 545-567.

Jamei, M., Villard, P., and Guiras (2013). "Shear failure criterion based on experimental and modeling results for fiber-reinforced clay." *International Journal of Geomechanics*, Vol. 13, No. 6, pp. 882-893, DOI: 10.1061/(ASCE)GM.1943-5622.0000258.

Karimpour-Fard, M., Machado, S. L., Shariatmadari, N., and Noorzad, A. (2011). "A laboratory study on the MSW mechanical behavior in triaxial apparatus." *Waste Management*, Vol. 31, No. 8, pp. 1807-1819, DOI: 10.1016/j.wasman.2011.03.011.

Kavazanjian, E. Jr., Matasovic, N., Bonaparte, R., and Schmertmann, G. R. (1995). "Evaluation of MSW properties for seismic analysis." *Geoenvironment 2000*, Geotechnical Special Publiction No. 46, pp. 1126-1141.

Kölsch, F., Fricke, K., Mahler, C., and Damanhuri, E. (2005). "Stability of landfills-The Bandung dumpsite disaster." In *Proceedings of the 10th International Waste Management and Landfill Symposium*, pp. 3-7 October 2005, Cagliari, Italy.

Machado, S. L., Carvalho, M. F., and Vilar, O. M. (2002). "Constitutive model for municipal solid waste." *Journal of Geotechnical and Geoenvironmental Engineering*, Vol. 128, No. 11, pp. 940-951, DOI: 10.1061/(ASCE) 1090-0241 (2002) 128:11(940).

Merry, S. M., Kavazanjian, E. Jr., and Fritz, W. U. (2005). "Reconnaissance of the July 10, 2000, Payatas landfill failure." *Journal of Performance of constructed Facilities*, Vol. 19, No. 2, pp. 100-107, DOI: 10.1061/(ASCE) 0887-3828 (2005)19:2 (100).

Michalowski, R. L. and Cermak, J. (2002). "Strength anisotropy of fiber-reinforced sand." *Computers and Geotechnics*, Vol. 29, No. 4, pp. 279-299, DOI: 10.1016/S0266-352X(01)00032-5.

Mofiz, S. A., Islam, M. N., Fratta, D., Puppala, A. J., and Munhunthan, B. (2010). "Modeling and numerical analysis of expansive soil in stress path tests." *In Proceedings of GeoFlorida 2010: Advances in analysis, modeling and design*, West Palm Beach, Florida, USA, 20-24 February 2010. (pp. 747-756).

Nayebi, A., Shariatmadari, N., Tehrani, M. H. H., and Oskouie, P. (2011). "Influence of aging on the mechanical behavior of Municipal

Solid Waste." *Geotechnical Risk Assessment and Management-Proceedings of the GeoRisk, ASCE, 2011 Conference*, pp. 696-703, DOI: 10.1061/41183(418)71.

Oztoprak, S. and Bolton, M. D. (2013). "Stiffness of sands through a laboratory database." *Geotechniqe*, Vol. 63, No. 1, pp. 54-70, DOI: org/10.1680/geot.10.P.078.

Pelkey, S. A., Valsangkar, A. J., and Landva, A. (2001). "Shear displacement dependent strength of municipal solid waste and its major constituents." *Geotechnical Testing Journal*, Vol. 24, No. 4, pp. 381-390, DOI: 10.1031/(ASTM) 0149-6155(2001)24:4(381).

Ple, O. and Le, T. N. H. (2012). "Effect of polypropylene fiber-reinforcement on the mechanical behavior of silty clay." *Geotixtiles and Geomembrances*, Vol. 32, No. 2, pp. 111-116, DOI: 10.1016/j.geotexmem. 2011.11.004.

Reddy, K. R., Hettiarachchi, H., Gangathulasi, J., Parakalla, N., and Bogner, J. E. (2009). "Geotechnical properties of fresh municipal solid waste at Orchard Hills Landfills, USA." *Waste Management*, Vol. 29, No. 2, pp. 952-959, DOI: 10.1016/j.wasman.2008.05.001.

Reddy, K. R., Hettiarachchi, H., Gangathulasi, J., and Bogner, J. E. (2011). "Geotechnical properties of municipal solid waste at different phases of biodegradation." *Waste Management*, Vol. 31, No. 11, pp. 2275-2286, DOI: 10.1016/j.wasman.2011.06.002.

Singh, M. K., Sharma, J. S., and Fleming, I. R. (2009). "Shear strength testing of intact and recompacted samples of municipal solid waste." *Canadian Geotechnical Journal*, Vol. 46, No. 10, pp. 1133-1145, DOI: 10.1139/T09-052

Tu, F. and Qian, X. (2008). "Unit weight, water content and specific gravity of municipal solid waste in China and United States." *Chinese Journal of Rock Mechanics and Engineering*, Vol. 27, Supp. 1, pp. 3075-3081.

Vilar, O. M. and Carvalho, M. F. (2004). "Mechanical properties of municipal solid waste." *Journal of Testing and Evaluation*, Vol. 32, No. 6, pp. 438-449, DOI: 10.1520/JTE11945.

Zekkos, D. (2005). "Evaluation of static and dynamic properties of Municipal Solid Waste." *Ph.D. Dissertation*, Depart. Of Civil and Environ. Engrg., Univ. of CalifoRnia, Berkley, Fall.

Zekkos, D., Athanasopoulos, G. A., Bray, J. D., Grizi, A., and Theodoratos, A. (2010). "Large-scale direct shear testing of municipal solid waste." *Waste Management*, Vol. 30, No. 8, pp. 1544-1555, DOI: 10.1016/j.wasman.2010.01.024.

Zekkos, D., Bray, J. D., and Riemer, M. F. (2012). "Drained response of municipal solid waste in large-scale triaxial shear testing." *Waste Management*, Vol. 32, No. 10, pp. 1873-1885, DOI: 10.1016/j.wasman.2012.05.004.

Zhan, T. L., Chen, Y. M., and Ling, W. A. (2008). "Shear strength characterization of municipal solid waste at the Suzhou landfill, China." *Engineering Geology*, Vol. 97, No. 3, pp. 97-111, DOI: 10.1016/j.enggeo.2007.11.006.